Molecules and Cells

NCAPH Stabilizes GEN1 in Chromatin to Resolve Ultra-Fine DNA Bridges and Maintain Chromosome Stability

Jae Hyeong Kim[1], Yuna Youn[1], and Jin-Hyeok Hwang[1,2,*]

[1]Department of Internal Medicine, Seoul National University Bundang Hospital, Seongnam 13620, Korea, [2]Department of Internal Medicine, Seoul National University College of Medicine, Seoul 03080, Korea
*Correspondence: woltoong@snu.ac.kr
https://doi.org/10.14348/molcells.2022.0048
www.molcells.org

Repairing damaged DNA and removing all physical connections between sister chromosomes is important to ensure proper chromosomal segregation by contributing to chromosomal stability. Here, we show that the depletion of non-SMC condensin I complex subunit H (NCAPH) exacerbates chromosome segregation errors and cytokinesis failure owing to sister-chromatid intertwinement, which is distinct from the ultra-fine DNA bridges induced by DNA inter-strand crosslinks (DNA-ICLs). Importantly, we identified an interaction between NCAPH and GEN1 in the chromatin involving binding at the N-terminus of NCAPH. DNA-ICL activation, using ICL-inducing agents, increased the expression and interaction between NCAPH and GEN1 in the soluble nuclear and chromatin, indicating that the NCAPH–GEN1 interaction participates in repairing DNA damage. Moreover, NCAPH stabilizes GEN1 within chromatin at the G2/M-phase and is associated with DNA-ICL-induced damage repair. Therefore, NCAPH resolves DNA-ICL-induced ultra-fine DNA bridges by stabilizing GEN1 and ensures proper chromosome separation and chromosome structural stability.

Keywords: chromosomal stability, condensin, DNA inter-strand crosslink, DNA repair, GEN1, NCAPH

INTRODUCTION

Repairing damaged DNA and removing all physical connections between sister chromosomes prior to anaphase is important for proper chromosome separation to ensure genomic stability. DNA interstrand cross-links (ICLs) induce the stalling of replication forks and DNA breaks (Bredberg et al., 1982; Dardalhon and Averbeck, 1995; De Silva et al., 2000; McHugh et al., 2000), and ICLs repair proceeds through the formation of double-strand breaks (DSBs) (Bessho, 2003; De Silva et al., 2000; McHugh et al., 2000). Immunodetection of phosphorylated histone H2AX (γ-H2AX) at Serine 139 is commonly used to visualize ICL processing and DSB induction in the cell nucleus (Niedernhofer et al., 2004; Redon et al., 2002; Rothfuss and Grompe, 2004; Thiriet and Hayes, 2005).

Homologous recombination (HR) is essential for the correct repair of ICLs and DSBs. HR causes the formation of four-way intermediate DNA structures, called Holliday junctions (HJs), that must be resolved to allow for chromosomal separation (Holliday, 2007; Li and Heyer, 2008). HJ resolvases are needed to resolve recombination intermediates to ensure proper chromosome segregation at mitosis. The BTR complex (BLM-TopoIIIa-RMI1/2), SLX–MUS complex (SLX1-SLX4 and MUS81-EME1), and GEN1 are three pathways that facilitate the dissolution of HJs in human cells (Sarbajna et al., 2014). The nucleolytic resolution of the main HJs is regulated by the

Received 25 March, 2022; revised 11 July, 2022; accepted 17 July, 2022; published online 11 November, 2022

eISSN: 0219-1032
©The Korean Society for Molecular and Cellular Biology.
This is an open-access article distributed under the terms of the Creative Commons Attribution-NonCommercial-ShareAlike 3.0 Unported License. To view a copy of this license, visit http://creativecommons.org/licenses/by-nc-sa/3.0/.

SLX4 complex (SLX4-SLX1/MUS81-EME1 and XPF-ERCC1) (Chen et al., 2001; Ciccia et al., 2003; Fekairi et al., 2009) and GEN1 (Ip et al., 2008), which determine whether crossover or non-crossover occurs. Yen1 is the yeast ortholog of human GEN1. The phosphorylation of S679 in Yen1 overlaps the nuclear localization signal, which inhibits nuclear import (Blanco et al., 2014; Eissler et al., 2014; Kosugi et al., 2009). Thereafter, Yen1 is activated by Cdc14 phosphatase, resulting in nuclear entry and enzymatic activation. Resolvase activity resolves the remaining HJs and ensures accurate DNA isolation (Blanco et al., 2014; Eissler et al., 2014). Although Mus81 and Yen1 in yeasts are sequentially activated by phosphorylation events, their activities do not overlap (Matos et al., 2011). In humans, GEN1 also reportedly reaches the chromatin, following nuclear envelope breakdown (Hustedt and Durocher, 2016) at the last stage of mitosis. However, unlike the mechanism that relies on Yen1 phosphorylation in yeast, the translocation of GEN1 is exclusively regulated by nuclear export signals (Chan and West, 2014). GEN1-deficient cells show increased chromosome missegregation, micronucleus formation, and genome instability, suggesting that GEN1 is essential for genome maintenance and proper chromosome segregation (Sarbajna et al., 2014; Wechsler et al., 2011).

Proper chromatin fiber condensation into the highly ordered structure of the mitotic chromosomes is crucial for achieving the equal segregation of sister chromatids until final physical cell division. During the course of the cell cycle, condensin I and II regulate mitotic chromosome compaction and resolution in different ways (Ono et al., 2003). The majority of higher eukaryotes, including humans, have two condensins, condensin I and condensin II. These two condensins share the same SMC2 and SMC4, and also contain non-SMC components with other kleisin subunit and HEAT repeat subunit pairs. Condensin I consists of CAP-H, -D2, and -G and condensin II consists of CAP-H2, -D3, and -G2. NCAPH is one of the non-SMC subunits of condensin I (Hirano, 2012; 2016; Thadani et al., 2012), which acts on chromosomes during mitosis, mostly in the cytoplasm during interphase, and occasionally during nuclear localization (Ono et al., 2003). Further, condensin I plays numerous other roles such as in DNA repair and in the epigenetic regulation of transcription (Chen et al., 2004; Dej et al., 2004). In particular, condensin I was reported to repair DNA single-strand breaks by binding to the PARP-1-XRCC-1 complex (Heale et al., 2006). During meiosis in yeasts, condensin is required for resolving recombination-dependent chromosome linkages (Yu and Koshland, 2003). Similarly, condensin is not associated with the export of ribosomal DNA breaks in the nucleus but rather facilitates the timely repair of meiotic DSBs (Li et al., 2014). Additionally, previous studies on NCAPH have shown that NCAPH-knockdown cells are arrested in the S and G2/M-phase; chromosomal aberrations and DNA damage are caused by the Chk1/Chk2 signaling pathways and play an essential role in the complete condensation of the chromosomes (Kim et al., 2019).

Here, we found that NCAPH regulates recovery from DNA damage-induced cell cycle arrest in both pancreatic cancer MIA PaCa-2 cells and human epithelial kidney HEK293 cells and restricts the formation of ultra-fine DNA bridge (UFB)-associated entanglement structures in sister chromosomes, thereby ensuring accurate chromosome separation. DNA-ICL induction, G2/M-phase arrest, UFB formation, chromosome segregation errors, and cytokinesis failure were observed in NCAPH-depleted cells. Interestingly, NCAPH interacted with GEN1, and the NCAPH–GEN1 interaction was enhanced following the induction of DNA-ICLs. Collectively, it was observed that NCAPH is closely related to GEN1 and is critical for the localization of GEN1 at sites of DNA damage. Therefore, NCAPH plays an important role in the recruitment and stabilization of GEN1 in chromatin to repair DNA damage, such as DNA-ICL, and maintain chromosomal stability.

MATERIALS AND METHODS

Cell culture, cell cycle synchronization

MIA PaCa-2 (CRL-1420) human pancreatic cancer cell lines and HEK293 (CRL-1573) human kidney cell lines were obtained from the American Type Culture Collection (ATCC, USA). Cells were grown in high-glucose Dulbecco's modified Eagle's (DMEM) medium. Cell culture mediums were used including 100 U/ml penicillin, 100 μg/ml streptomycin, and 10% fetal bovine serum (Gibco Life Technologies, USA). To synchronize cells at late G1-phase (near the G1-S boundary), a double thymidine arrest/release experiments was performed (Whitfield et al., 2000). For a double thymidine block experiments, cells were synchronized with 2 mM thymidine (1-[2-deoxy-β-d-ribofuranosyl]-5-methyluracil) (Sigma, USA). After the second thymidine treatment, fresh medium was replaced and samples were taken at each time point (Chen and Deng, 2018).

Small interfering RNA (siRNA) or plasmid DNA transfection

Cells were transfected with NCAPH siRNA using the Lipofectamine RNAiMAX transfection reagent (Invitrogen, USA) according to manufacturer's instructions. NCAPH siRNA was synthesized as 5'-AAU AGU UCU GUG UAA GUG C-3' and 5'-GCA CUU ACA CAG AAC UAU U-3'. NCAPH siRNA (Georges et al., 2008) and control siRNA were provided by Cosmo Bio (Cosmo Genetech, Korea). For DNA transfection, the cells were transfected with Flag vector, Flag-tagged full length NCAPH, three domains of NCAPH, GST vector and GST-tagged full length GEN1 using the Lipofectamine 3000 transfection reagent (Invitrogen) according to manufacturer's instructions.

Fluorescence-assisted cell sorting (FACS) analysis

For measurements of cell cycle and DNA content, cells were collected, and washed in 1× phosphate-buffered saline (PBS) and fixed with 70% ethanol at 4°C overnight before being stained with PI (propidium iodide; Sigma) 50 μg/ml and 100 U RNase (ribonuclease A from bovine pancreas; Sigma). The analysis rate was 300-500 cells/s. Clones were assessed in three independent runs. Analysis was performed using FACS Calibur (BD Biosciences, USA) according to standard protocols.

Cytoplasmic, soluble nuclear fraction, and chromatin fractions

Cytoplasmic, soluble nuclear, and chromatin proteins were divided with the NE-PER Nuclear and Cytoplasmic Extraction Reagents (#78835; Thermo Fisher Scientific, USA). Briefly, cell pellets were lysed with CERI buffer, and forceful vortex was applied for 15 s and incubated on ice for 10 min. Next, CER II buffer was added to the samples was shaken strenuously for 5 s and incubated for 1 min on ice (cytoplasmic fraction). After centrifugation at 16,000 × *g* for 5 min, the pellet was re-suspended with nuclear extraction reagent and incubated on ice for 40 min with intermittent vortex. Nuclear fractions were collected after centrifugation at 16,000 × *g* for 10 min (soluble nuclear fraction). The pellet was washed two times with 1× PBS. Then, the cell pellet was re-suspended in radio immunoprecipitation assay (RIPA) lysis buffer (Beyotime Biotech, China) and incubated on ice for 40 min and then sonicated for 30 s, it was turned on for 2 s and then turned off for 3 s repeatedly (chromatin fraction). All buffers except CERII buffer were supplemented with PMSF, protease inhibitor, and phosphatase inhibitor cocktails. Fractions were supplemented with 4× (for western blot) or 2× (for immunoprecipitation) laemmli sample buffer (contains 10% or 5% 2-mercaptoethanol; Bio-Rad, USA) and boiled for 5 min at 95°C, and were examined using western blotting analysis or immunoprecipitation.

Western blot and antibodies

Whole cells were washed once with cold 1× PBS and then collected. Cells were homogenized with 1× RIPA lysis buffer, and protein concentration was determined using BCA Protein Assay Kit (Pierce, USA). Protein extracts were re-suspended in 4× sample buffer containing 10% of 2-mercaptoethanol, boiled for 5 min, and subjected to 8%-15% sodium dodecyl sulfate-polyacrylamide gel electrophoresis and electrotransferred to a Trans-blot nitrocellulose membrane (Whatman International, UK). Transferred membranes were blocked in 5% skim milk in TBST buffer (10 mM Tris [pH 8.0], 150 mM NaCl, 0.05% Tween 20) and incubated with primary antibodies at 4°C overnight. The primary antibodies were purchased from commercial sours: anti-NCAPH (Novus Biological, USA), anti-NCAPG (Bethyl Laboratories, USA), anti-NCAPH2 (Bethyl Laboratories), anti-NCAPD3 (Proteintech, China), anti-GEN1 (Novus Biological), anti-MUS81 (Novus Biological), anti-Cyclin A2 (Cell Signaling Technology, USA), anti-Histone H3 (Abcam, USA), anti-phosphorylated Histone H3 at pS10 (pS10 histone H3) (Abcam), anti-phosphorylated H2AX at S139 (p-H2AX) (Millipore, USA), anti-GAPDH (Thermo Fisher Scientific), anti-LMNA (Bethyl Laboratories), anti-alpaha Tubulin (Abcam), and anti-β-actin (Sigma). Protein expressions analyzed chemiluminescent signals activated by SuperSignal West Pico Chemiluminescent Substrate (Pierce) reacted with horse radish peroxidase tagged secondary antibodies (Jackson ImmunoResearch, USA).

Immunoprecipitation

Flag-tagged full-length NCAPH and GEN1 proteins were expressed in HEK293 cells and purified with FLAG M2 monoclonal antibody affinity gel (Sigma) according to manufacturer's instructions. GST-tagged full-length GEN1 protein was expressed in HEK293 cells and purified with Glutathione-Sepharose 4B (Thermo Fisher Scientific) according to manufacturer's instructions. HEK293 cells transfected with three truncation domain constructs Flag-tagged-NCAPH (N-NCAPH [1–250], M-NCAPH [251–500], and C-NCAPH [501-741]) or control vector and then purified with Glutathione-Sepharose 4B or FLAG M2 monoclonal antibody affinity gel (Sigma). The primary antibodies were acquired from commercial sours: anti-Flag (Sigma), anti-GST (Cell Signaling Technology), anti-NCAPH (Novus Biological), anti-NCAPD2 (Bethyl Laboratories), anti-GAPDH (Thermo Fisher Scientific), anti-LMNA (Bethyl Laboratories). The ATM-kinase inhibitor (KU-55933) was acquired from Sigma.

Immunofluorescence

Cells were grown on Thermo Fisher Scientific Nunc Lab-Tek II Chamber Slides & trade, fixed with 4% paraformaldehyde for 15 min or PTEM buffer containing 20 mM PIPES (pH 6.8), 0.2%. Triton X-100, 10 mM EGTA, and 4% paraformaldehyde for 10 min, and permeabilized with 0.5% Triton X-100 for 5 min. The fixed cells were incubated for 1 h with % bovine serum albumin and then incubated overnight at 4°C with primary antibody, then the next day add the fluorophore-conjugated secondary antibody for 2 h. Samples were mounted in Vectashield Mounting Medium with DAPI (Vector laboratories, USA), and the results were observed under a confocal microscope (Zeiss LSM 710 or LSM 800, software ZEN; Zeiss, Germany). The primary antibodies were acquired from commercial sours: anti-NCAPH (Novus Biological), anti-GEN1 (Novus Biological), anti-p-H2AX (Millipore), anti-CREST (ImmunoVision, USA), anti-GFP (Invitrogen), and anti-alpha Tubulin (Abcam).

Lentivirus expression of NCAPH and site-directed mutagenesis

The NCAPH expression vector was constructed as a pLenti6/V5-DEST lentiviral vector and was purchased through Addgene (#31214). To produce siRNA-resistant mutant NCAPH (siR-NCAPH), the mutants (siR-NCAPH forward primer: 5'-CAA AGA AGA AGC ACTT GCA TAG GAC TAT TGA GCA GAA C-3', siR-NCAPH reverse primer: 5'-GTT CTG CTC AAT AGT CCT ATG CAA GTG CTT CTT CTT TG-3') were generated using QuikChange II Site-Directed Mutagenesis Kit (Stratagene, USA). To produce lentivirus from a NCAPH lentiviral vector, 293FT cells cultured in a 100 mm plate were co-transfected with 3 μg of NCAPH ranging from 4 μg using 3 μg of the packaging vectors (pRsv-REV, pMDLg/pRRE and pMD2.G). Six hours after transfection, cells were changed with MEM medium supplemented with 10% fetal bovine serum but not antibiotics. Another 72 h later, the medium was centrifuged at 500 × *g* for 10 min and decanted into another tube. One volume of Lenti-X Concentrator solution (Clontech, USA) with tree volumes of the collected-medium were mixed and incubated at 4°C for 40 min. Next, mixture centrifuged 1,500 × *g* for 45 min and then removes the supernatant. The pellet was re-suspended in DMEM with 10% fetal bovine serum, and virus was aliquoted and stored at –80°C.

Statistical analysis

All data will be represented central tendency obtained in form two or three independent replicate experiments. The data of the experiments were statistically analyzed using GraphPad Prism 5 (GraphPad Software, USA) and presented as mean ± SEM. Statistical analysis was performed using unpaired *t*-tests, one-way or two-way ANOVA followed by Bonferroni's multiple comparison analysis tests.

Data availability statement

The authors declare that all relevant data supporting the findings of the study are available within the manuscript, figure, and supplementary information, and are available from the respective authors upon reasonable request.

RESULTS

NCAPH response to DNA-ICLs-induced DSB formation

First, we determined whether NCAPH localization/enrichment in the cytoplasm, nuclear and chromatin fractions is altered during cell cycle progression under DNA-ICL induction with mitomycin C (MMC) and cisplatin, which are DNA damage-inducing agents (Deans and West, 2011). Cell cycle progression proceeded with a double thymidine block. As the second thymidine block treatment was performed, DNA damage was induced by MMC, and time-dependent harvesting was performed for flow cytometry and western blotting analyses (Fig. 1A). Dimethyl sulfoxide (DMSO)-treated cells stopped at the G1/S-phase boundary 0 h, the S-phase population increased at 4 h, and the G/2M-phase population increased at 8 h after release from the second thymidine treatment (Supplementary Figs. S1A and S1B). However, the S-phase population of MMC-treated cells was significantly increased after release from the second thymidine treatment (Supplementary Figs. S1A and S1B). To confirm the occurrence of DSBs during DNA-ICL repair, the formation of γH2AX (p-H2AX), the phosphorylated Ser-139 residue of H2AX, was monitored. In the absence of MMC, NCAPH was weakly expressed in chromatin$^+$ in the late G1-phase at 0 h after release from the second thymidine treatment. However, as the cell cycle progressed into the G2/M-phase, NCAPH localization/enrichment in the chromatin$^+$ increased (Fig. 1B, –MMC). Low expression levels of p-H2AX were detected throughout cell cycle progression. However, p-H2AX expression and NCAPH localization/enrichment in the chromatin$^+$ were increased significantly by MMC-induced DNA-ICLs from 0 to 8 h after release from the second thymidine treatment (Fig. 1B, +MMC). Immunofluorescence specifically confirmed that NCAPH expression in MMC-induced DNA-ICLs occurred in parallel with p-H2AX accumulation (Fig. 1C). Intranuclear expression levels of NCAPH were also increased by MMC-induced DNA-ICLs (Fig. 1D). Thus, it was confirmed that NCAPH localization/enrichment in the chromatin fraction was increased by DSBs caused by DNA-ICLs.

The effects of cisplatin- and MMC-induced DNA-ICLs and NCAPH depletion on the cell cycle were analyzed based on flow cytometry and western blotting analyses. Cells were transfected with control and NCAPH siRNAs and exposed to cisplatin or MMC for 24 h. The flow cytometry results indicated that the G2/M-phase population increased in NCAPH-depleted cells, and the G2/M-phase population increased more in cisplatin-treated NCAPH-depleted cells (Figs. 1E and 1F). Upon MMC treatment, control cells increased in the S-phase population, whereas NCAPH-depleted cells increased in the G2/M-phase population (Figs. 1E and 1F). When cisplatin or MMC was used to induce DNA-ICLs in NCAPH-depleted cells, the expression levels of cyclin A2 and p-H2AX were increased compared with those in the control cells (Fig. 1G). These results suggest that NCAPH plays an essential role in the repair of cisplatin- or MMC-induced DNA-ICLs to ensure proper mitosis progression.

Abnormal phenomena caused by UFB induction in NCAPH-depleted cells

To explore the effect of unresolved recombinant intermediates caused by DNA-ICLs on mitosis, the cells were transfected with control and NCAPH siRNAs and exposed to cisplatin for 1 h. After 24 h, immunofluorescence was performed using anti-PLK1 interacting checkpoint helicase (PICH). The PICH, an SNF2-family DNA translocase, is localized in UFBs and is required for chromosome organization and proper chromosome segregation. PICH is essential for the progression of UFBs via the recruitment of UFB-associated proteins and the mediation of UFB resolution during mitosis (Chan et al., 2009; Chanboonyasitt and Chan, 2021; Wang et al., 2010; 2008). Following the induction of DNA-ICLs by cisplatin, approximately 16% of the NCAPH-depleted cells were observed to be in late anaphase telophase, whereas only about 4% of the control cells were observed in this phase (Fig. 2A, left graph). The frequency of UFBs in late anaphase-telophase NCAPH-depleted cells increased significantly to about 66% compared to only 6.6% in the control group (Fig. 2A, middle graph). The number of UFBs observed in NCAPH-depleted cells was approximately 3.3, whereas UFBs were observed only rarely in the control cells (Fig. 2A, right graph).

Immunofluorescence analyses were performed using DNA, CREST (a centromere marker), and α-tubulin to investigate defective abnormal chromosome separation. Following DNA-ICL induction by cisplatin, approximately 75% of the NCAPH-depleted cells in the late anaphase telophase stage showed abnormal chromosome separation, such as chromosome bridges and chromosome lagging (Fig. 2B). In contrast, only 6.6% of control cells in this stage showed abnormal chromosome separation. We further examined the effect of NCAPH depletion and cisplatin on cytokinesis during the cell division process. In the absence of cisplatin treatment, 31.9% of the NCAPH-depleted cells showed cytokinesis failure, as opposed to only 5% of the control group. In the presence of cisplatin, 58.8% cytokinesis failure was observed in NCAPH-depleted cells compared with only 10.1% observed in the control group. Thus, there was a noteworthy difference between the extent of cytokinesis failure among NCAPH-depleted cells depending on the presence or absence of cisplatin (Fig. 2C). These results indicate that defects in NCAPH exacerbate chromosome segregation errors and cytokinesis failure owing to sister-chromatid intertwinement, a distinct form of UFB produced by cisplatin-induced DNA-ICLs.

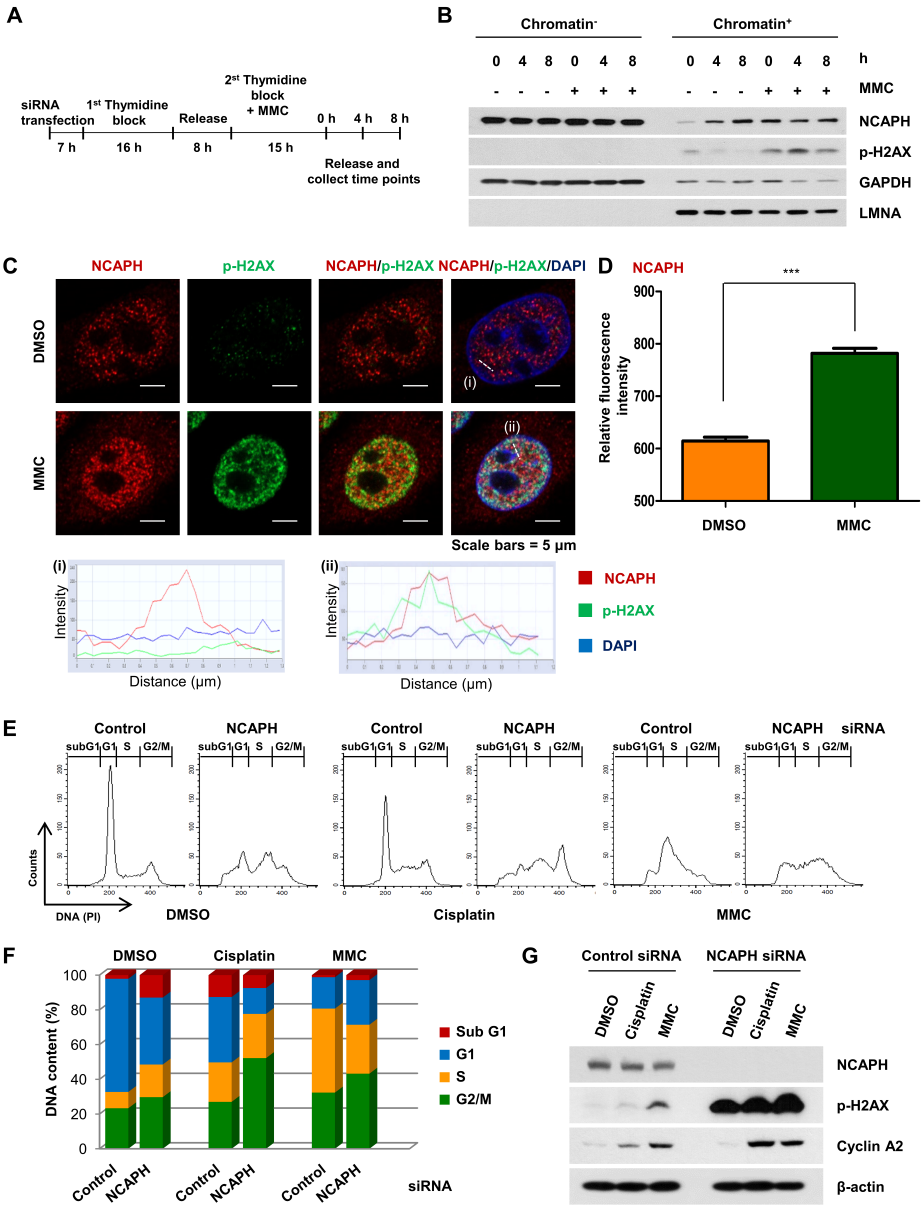

Fig. 1. Response of NCAPH by DNA-ICL induction using MMC and cisplatin treatment. (A) Introduction to a brief overview of the procedure for double thymidine block synchronization. (B) MIA PaCa-2 cells were treated with 2 μM MMC from the second thymidine treatment, and then analyzed at separate time points ranged from 0, 4, and 8 h after release of second thymidine treatment. Comparison of the chromatin$^-$ and chromatin$^+$ fractions of MIA PaCa-2 cells. Western blotting analysis was performed to show protein expression levels of NCAPH, p-H2AX, and LaminA/C (LMNA); nuclear marker. Glyceraldehyde-3-phosphate dehydrogenase (GAPDH); cytoplasmic marker. (C) MIA PaCa-2 cells were treated with 2 μM MMC in the second thymidine treatment and then subjected to immunofluorescence analysis at 8 h after release from the second thymidine treatment. p-H2AX (green) and NCAPH (red) fluorescence pattern was observed by confocal microscopy. DNA was stained with DAPI (blue). Scale bars = 5 μm. (i and ii) Colocalization analysis of NCAPH (red curve) and p-H2AX (green curve) with DAPI (blue curve). The fluorescence intensity profiles of NCAPH and p-H2AX show the fluorescence distribution across the dotted line (x-axis). The fluorescence intensity is plotted along the y-axis. (D) Measurements of the mean fluorescence intensity of NCAPH. For precise quantification, more than 100 cell images captured by fluorescence microscopy at least three different fields. Values are represented in the form of mean ± SEM. Statistical analysis of data was obtained by unpaired *t*-tests. ***$P < 0.0001$. (E) MIA PaCa-2 cells were transfected with control and NCAPH siRNA, and treated with DMSO, 1 μg/ml cisplatin, or 2 μM MMC for 24 h. Analyze the cell cycle by flow cytometry. (F) Histogram bar graph visualize the percentages in cells in sub-G1 (red), G1 (blue), S (orange), and G2/M (green) phases. The experiments were performed in triplicate, repeated at least three times. The mean values of the results are presented. *$P < 0.005$, two-way ANOVA. (G) MIA PaCa-2 cells were transfected with control and NCAPH siRNA, and treated with DMSO, 1 μg/ml cisplatin, or 2 μM MMC for 24 h. The protein expression levels of NCAPH, p-H2AX, cyclin A2, and β-actin were measured by western blotting.

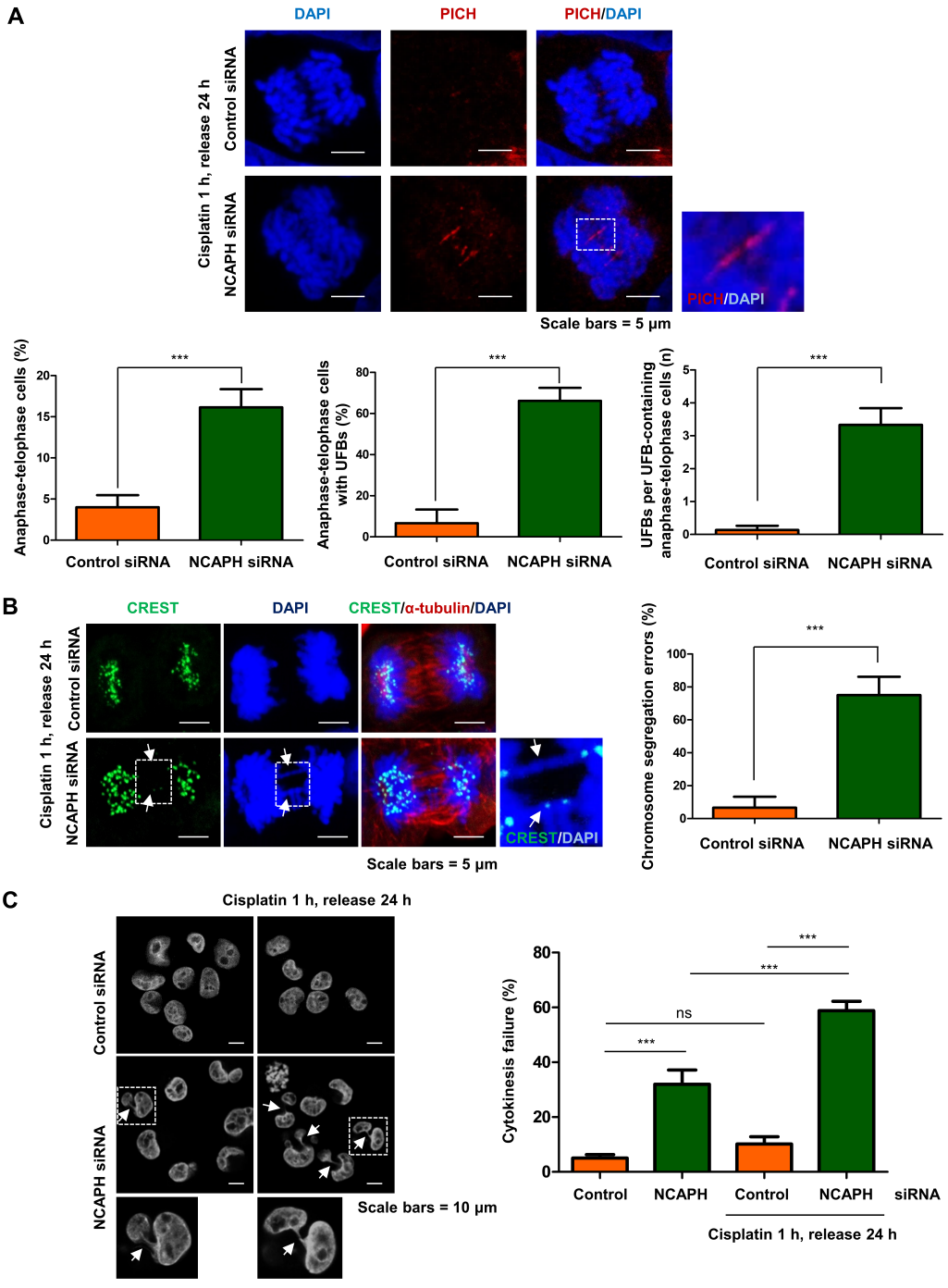

Fig. 2. NCAPH-depleted cells induce UFB formation, chromosome segregation errors, and cytokinesis failure by cisplatin-induced DNA-ICLs. (A) To confirm the formation of UFBs, HEK293 cells were transfected with control and NCAPH siRNA, and treated with 1 μg/ml cisplatin for 1 h. After 24 h, immunofluorescence was performed using anti-PICH. DNA was stained with DAPI (blue). Scale bars = 5 μm. For precise quantification, more than 300 cells captured images by fluorescence microscopy at least three independent experiments were analyzed. Values are represented in the form of mean ± SEM. Statistical analysis of data was obtained by unpaired *t*-tests. ***$P < 0.0001$. (B) HEK293 cells transfected with control or NCAPH siRNA were stained for CREST (green), α-tubulin (red), and DNA (blue). Scale bars = 5 μm. For precise quantification, more than 300 cells captured images by fluorescence microscopy at least three independent experiments were analyzed. Values are represented in the form of mean ± SEM. Statistical analysis of data was obtained by unpaired *t*-tests. ***$P < 0.0001$. (C) MIA PaCa-2 cells transfected with control or NCAPH siRNA were stained for DNA (gray). Scale bars = 10 μm. For precise quantification, more than 300 cells captured images by fluorescence microscopy at least three independent experiments were analyzed. Values are represented in the form of mean ± SEM. ***$P < 0.0001$; ns, not significant. Statistical analysis of data was obtained by one-way ANOVA followed by Bonferroni's multiple comparison analysis tests.

NCAPH interacts with GEN1 via DNA damage response

HR repairs DNA damage prompted by cisplatin-induced DNA-ICLs. To understand the mechanism underlying NCAPH regulation during DNA damage repair progression, we explored its relationship with MUS81 and GEN1 resolving enzymes (Bittmann et al., 2020; García-Luis et al., 2014; Grigaitis et al., 2020; Machín, 2020; Wyatt et al., 2013). To gain a better understanding of the relationship between NCAPH and HJ resolvases, we tested the hypothesis that NCAPH acts as a binding partner of GEN1 by investigating whether NCAPH interacts with GEN1. Binding among the Flag-tagged full-length NCAPH protein, another condensin I component, non-SMC condensin I complex subunit D2 (NCAPD2), endogenous GEN1, and MUS81 was analyzed via immunoprecipitation analysis. Exogenously expressed Flag-tagged full-length NCAPH interacted with both endogenous GEN1 and NCAPD2 but not with MUS81 (Fig. 3A). Immunoprecipitation confirmed the interaction between the Flag-tagged full-length GEN1 protein and endogenous NCAPH (Fig. 3B). Additionally, we analyzed the interaction between NCAPH and GEN1 by producing Flag-tagged full-length NCAPH (Flag-NCAPH) and glutathione S-transferase (GST)-tagged full-length GEN1 (GST-GEN1) and performing immunoprecipitation experiments. These results showed that exogenously expressed Flag-tagged full-length NCAPH interacted with GST-tagged full-length GEN1 (Fig. 3C). Furthermore, a double thymidine block followed by time-dependent harvesting was performed to analyze the expression patterns of NCAPH and the HJ resolvases with western blotting (Supplementary Fig. S2A). The expression levels of NCAPH and GEN1 in the chromatin^{+} increased during the G2/M-phase 8 h after release from the second thymidine treatment. In contrast, MUS81 expression in the chromatin^{+} increased only 4 h after release from the second thymidine treatment (Supplementary Fig. S2B). Immunofluorescence indicated that overexpressed GFP-tagged NCAPH localized with GEN1, confirming their presence in the same location in the nucleus (Supplementary Fig. S2C). In addition, immunofluorescence confirmed that GEN1 was co-expressed with p-H2AX in cells displaying MMC-induced DNA damage in a manner comparable to that of NCAPH, thereby demonstrating that GEN1 expression in the nucleus was increased by MMC-induced DNA damage (Supplementary Fig. S2D).

To analyze the signaling pathway involved in the interaction between NCAPH and GEN1, immunoprecipitation experiments of Flag-NCAPH and GST-GEN1 were performed using Ataxia telangiectasia mutated (ATM)-kinase inhibitor treatment, and the resulting fractions were divided into those with and without chromatin. The interaction of NCAPH and GEN1 in chromatin partially decreased under ATM-kinase inhibitor treatment (Fig. 3D). Immunoprecipitation assays using Flag-tagged-NCAPH (N-NCAPH [1-250], M-NCAPH [251-500], and C-NCAPH [501-741]) showed that the N-NCAPH bound strongly to GEN1 and that NCAPD2 bound strongly to the N-NCAPH (Figs. 3E and 3F). These results suggest that NCAPH and GEN1 form a close relationship, that N-NCAPH is important for binding GEN1 with other condensin components and that the ATM signaling pathway is partially involved in the NCAPH–GEN1 interaction.

Finally, we performed flow cytometry and immunoprecipitation experiments to test whether the interaction between NCAPH and GEN1 was altered by MMC-induced DNA damage. Cell cycle analysis revealed that DMSO-treated cells stopped at the G1/S-phase boundary at 0 h, the S-phase population increased after 4 h, and the G2/M-phase population increased after 8 h after release from the second thymidine treatment (Supplementary Figs. S1C and S1D). However, in MMC-treated cells the S-phase population increased 0-8 h after release from the second thymidine treatment (Supplementary Figs. S1C and S1D). In addition, the binding between NCAPH and GEN1 in the chromatin^{+} was significantly increased owing to MMC-induced DNA damage (Fig. 3G). Consequently, NCAPH interacts with GEN1 via a DNA damage response.

NCAPH is essential for GEN1 recruitment and stabilization in chromatin

To determine the effect of NCAPH on the chromatin localization of GEN1, NCAPH-depleted cells and control cells were double-blocked with thymidine (Fig. 4A). Preferentially, the cell cycle was analyzed 0-12 h after release from the second thymidine treatment (Fig. 4B). The S-phase population and cyclin A2 expression were more increased 4 h after release from the second thymidine treatment in NCAPH-depleted cells than in control cells. After 8 h, the G2/M-phase population and cyclin A2 and phospho-histone H3 (pS10 histone H3) expression were more increased in NCAPH-depleted cells than in control cells (Fig. 4C). Next, western blotting was performed after separation into the cytoplasmic, nuclear, and chromatin components. Although the expression of NCAPH and other condensin I components (NCAPG) in the cytoplasm, nucleus, and chromatin fractions were affected by NCAPH depletion, the components of condensin II (NCAPH2) were not (Fig. 4D). GEN1 expression in chromatin fraction was higher at 8 h than at 0 h after release from the second thymidine treatment (late G1-phase). However, GEN1 expression in the chromatin fraction was significantly reduced 8 h after release from the second thymidine treatment (G2/M-phase) owing to NCAPH depletion (Fig. 4D, Chr). Furthermore, GEN1 expression did not change significantly in the cytoplasm or nucleus (Fig. 4D, Cyt and Nuc). Following the induction of DNA-ICLs via MMC in NCAPH-depleted cells, p-H2AX expression was markedly increased compared with that in control cells. Although there was no significant alteration in GEN1 expression, colocalization between GEN1 and p-H2AX was significantly inhibited (Fig. 4E).

To clarify the involvement of NCAPH in the recruitment and stabilization of GEN1 in chromatin fraction, we conducted reconstitution experiments after NCAPH siRNA transfection. First, we produced lentiviral vector-expressing siRNA-resistant NCAPH (Lenti-siR-NCAPH) and performed reconstitution experiments (Fig. 5A). Next, the cells were separated into cytoplasm, nucleus, and chromatin fractions, and changes in the recruitment and stabilization of GEN1 to DNA damage sites were predicted by reconstruction experiments using western blotting analyses. The decrease in chromatin-specific GEN1 localization in NCAPH-depleted cells was restored by Lenti-siR-NCAPH treatment (Fig. 5B). In addition, the localization of

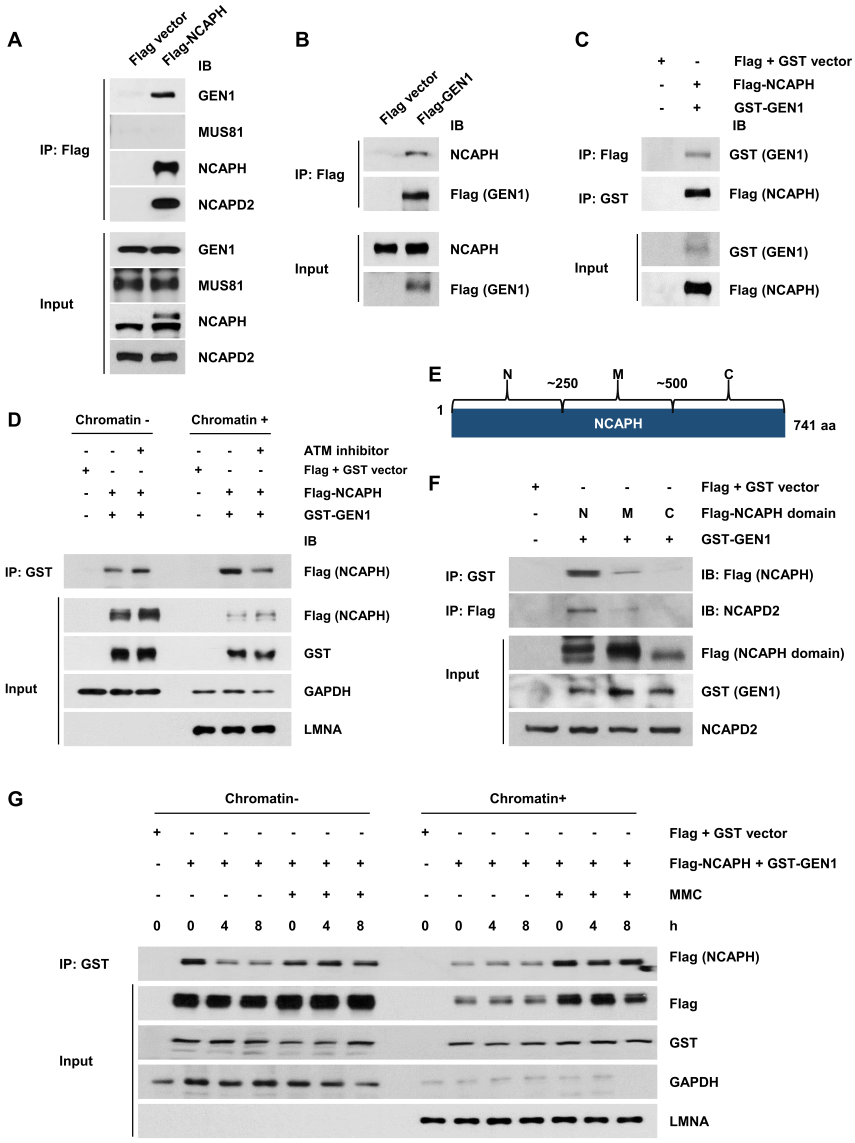

Fig. 3. NCAPH interacts with GEN1 to mediated DNA repair of MMC-induced DNA-ICLs. (A) HEK293 cells were transfected Flag-tagged full-length NCAPH or control vector. Total lysates in input and immunoprecipitated (IP) with anti-Flag M2 affinity gel, and then analyzed by immunoblotting (IB) with specific antibodies (GEN1, MUS81, NCAPH, and NCAPD2 antibodies). (B) HEK293 cells were transfected Flag-tagged full-length GEN1 or control vector. Total lysates in input and immunoprecipitated with anti-Flag M2 affinity gel, and then analyzed by immunoblotting with specific antibodies (NCAPH and Flag antibodies). (C) HEK293 cells were transfected Flag-tagged full-length NCAPH and GST-tagged full-length GEN1. Total lysates in input and immunoprecipitated with anti-Flag M2 affinity gel or Glutathione-Sepharose beads, and then analyzed by immunoblotting with specific antibodies (GST and Flag antibodies). (D) HEK293 cells were transfected Flag-tagged full-length NCAPH and GST-tagged full-length GEN1 with ATM-kinase inhibitor treatment for 24 h, and immunoprecipitation analysis. Comparison of the cytoplasmic and chromatin fractions of HEK293 cells prepared by lysis through chromatin fractionation. Total lysates in input and immunoprecipitated with Glutathione-Sepharose beads, and then analyzed by immunoblotting with specific antibodies (Flag, GST, GAPDH, and LMNA antibodies). (E) Diagram of full-length NCAPH and three truncation domain constructs (N-NCAPH [N], M-NCAPH [M], C-NCAPH [C]). Protein size is given in amino acids (aa). (F) HEK293 cells were transfected three domains of NCAPH and GST-tagged full-length GEN1. Total lysates in input and immunoprecipitated with anti-Flag M2 affinity gel or Glutathione-Sepharose beads, and then analyzed by immunoblotting with specific antibodies (Flag, GST, and NCAPD2 antibodies). (G) HEK293 cells were transfected Flag-tagged full-length NCAPH and GST-tagged full-length GEN1 and then treated with 2 μM MMC in the second thymidine treatment. Immunoprecipitation assay was performed at 0, 4, 8 h after release from the second thymidine treatment. Comparison of the cytoplasmic and chromatin fractions of HEK293 cells prepared by lysis through chromatin fractionation. Total lysates in input and immunoprecipitated with Glutathione-Sepharose beads, and then analyzed by immunoblotting with specific antibodies (Flag, GST, GAPDH, and LMNA antibodies). Flag-NCAPH, Flag-tagged full-length NCAPH; Flag-GEN1, Flag-tagged full-length GEN1; GST-GEN1, GST-tagged full-length GEN1.

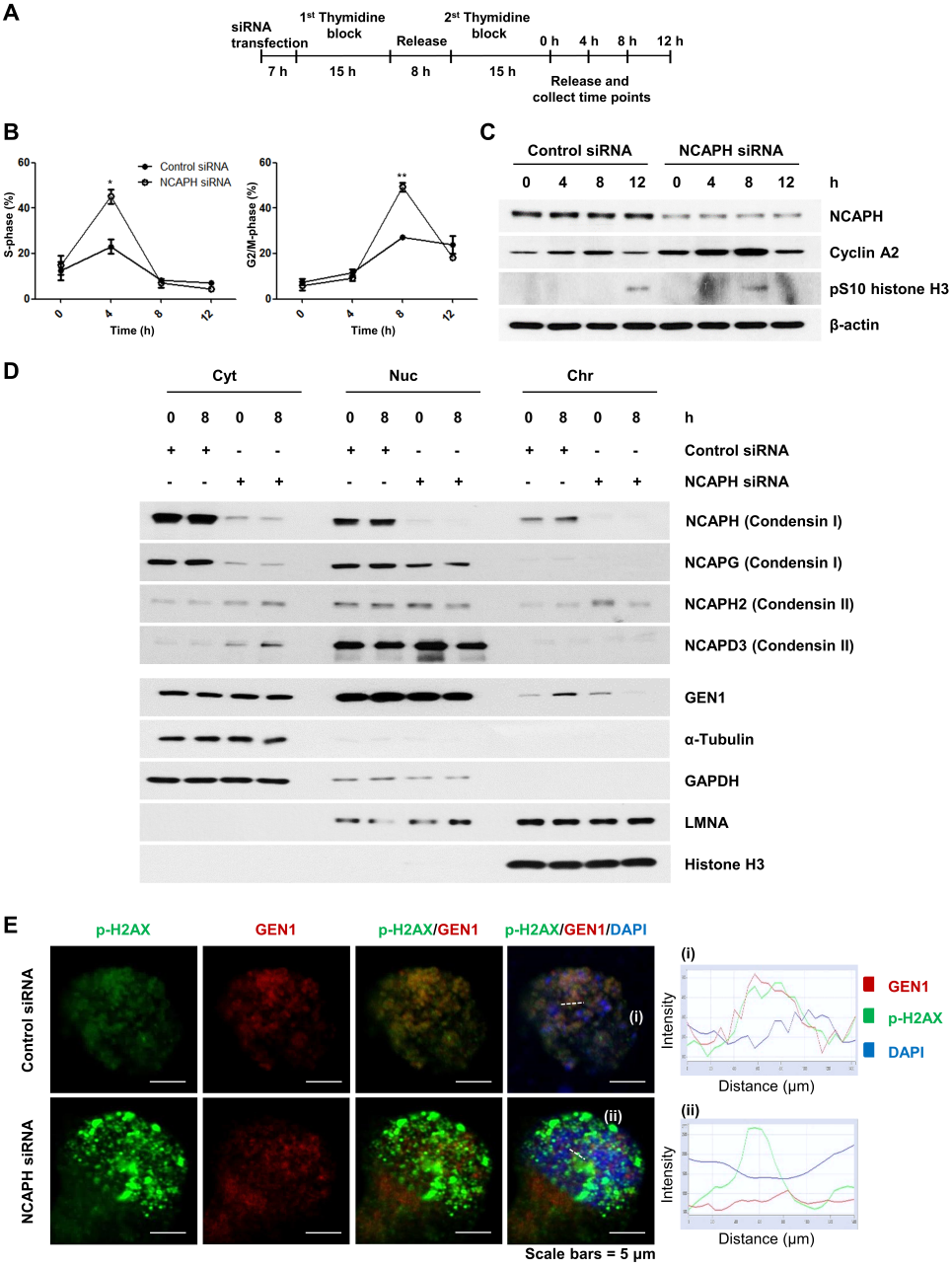

Fig. 4. NCAPH-depleted cells dramatically reduced GEN1 recruitment and stabilization in chromatin at G2/M-phase. (A) Introduction to a brief overview of the procedure for double thymidine block synchronization. (B) MIA PaCa-2 cells were transfected with control and NCAPH siRNA and double thymidine block synchronization was performed. The cells were analyzed for 0, 4, 8, and 12 h after release from the second thymidine treatment. Analyze the cell cycle by flow cytometry. Line graph visualize the percentages in cells in S and G2/M-phase population. Values represent mean ± SEM. $*P < 0.005$, $**P < 0.001$. Results were analyzed using unpaired *t*-tests. (C) The protein expression levels of NCAPH, cyclin A2, pS10 histone H3, and β-actin were measured by western blotting. (D) MIA PaCa-2 cells were transfected with control and NCAPH siRNA and double thymidine block synchronization was performed. The cells were analyzed for 0 and 8 h after release from the second thymidine treatment. Comparison of the Cyt (cytoplasmic), Nuc (soluble nuclear), and Chr (chromatin) fractions of MIA PaCa-2 cells prepared by lysis through chromatin fractionation experiments. Western blotting analysis was performed to show protein expression levels of NCAPH, NCAPG, NCAPH2, NCAPD3, GEN1, α-tubulin, GAPDH, LMNA, Histone H3. (E) MIA PaCa-2 cells were treated with 2 μM MMC in the second thymidine treatment and then subjected to immunofluorescence analysis at 8 h after release from the second thymidine treatment p-H2AX (green) and GEN1 (red) fluorescence pattern was observed by confocal microscopy. DNA was stained with DAPI (blue). Scale bars = 5 μm. (i and ii) Colocalization analysis of NCAPH (red curve) and p-H2AX (green curve) with DAPI (blue curve). The fluorescence intensity profiles of NCAPH and p-H2AX show the fluorescence distribution across the dotted line (x-axis). The fluorescence intensity is plotted along the y-axis.

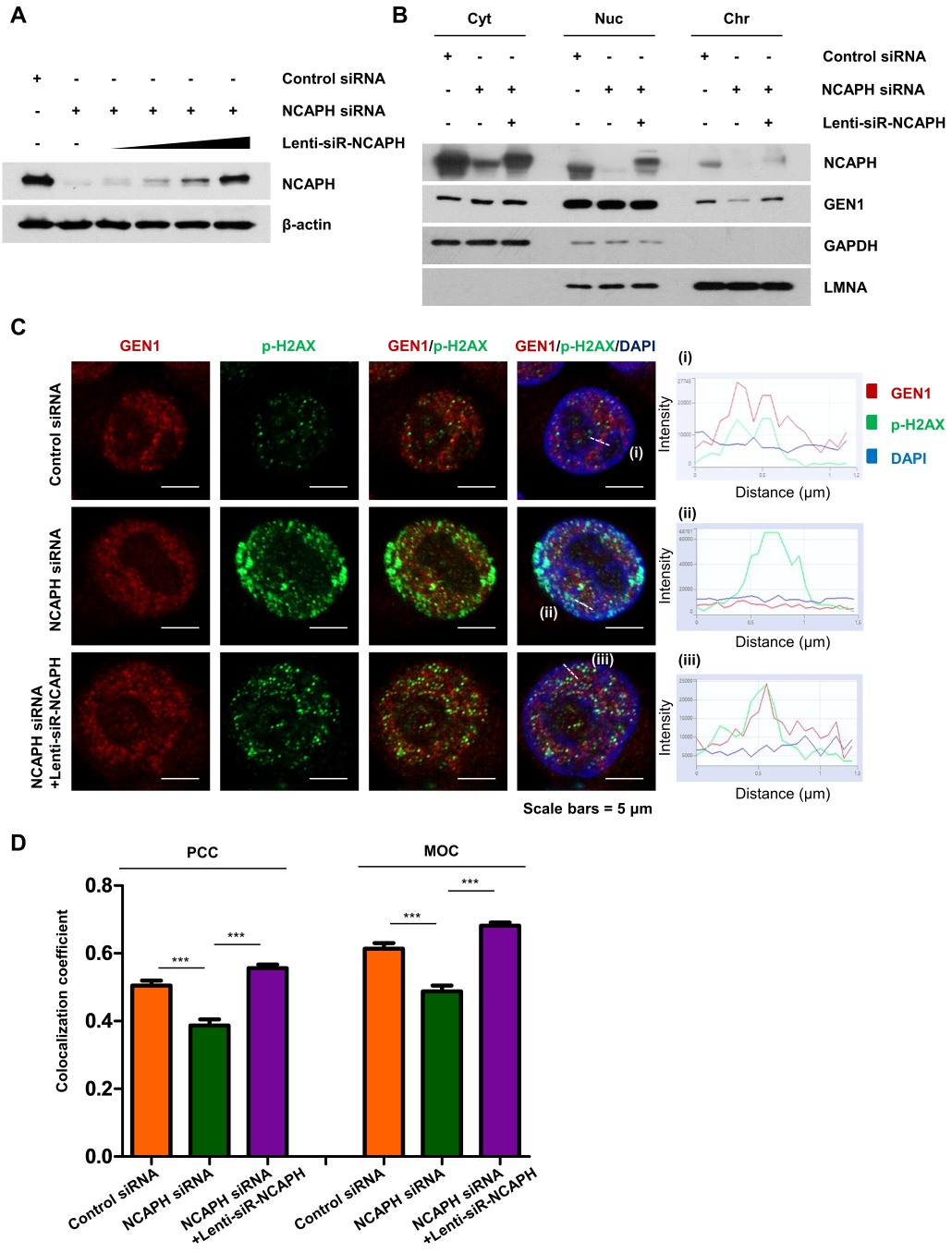

Fig. 5. NCAPH required for GEN1 recruitment and stabilization to chromatin. (A) Western blotting analysis of total cell lysates harvested after control and NCAPH siRNA transfection into MIA PaCa-2 cells and dose-dependent treatment of Lenti-siR-NCAPH. Western blotting analysis was performed to show protein expression levels of NCAPH and β-actin. (B) Comparison of the Cyt (cytoplasmic), Nuc (soluble nuclear), and Chr (chromatin) fractions of MIA PaCa-2 cells prepared by lysis through chromatin fractionation experiments. Western blotting analysis was performed to show protein expression levels of NCAPH, GEN1, GAPDH, and LMNA. (C) MIA PaCa-2 cells were treated with or without Lenti-siR-NCAPH after transfection with control and NCAPH siRNA. After 48 h, p-H2AX (green) and GEN1 (red) fluorescence patterns was observed by confocal microscopy. DNA was stained with DAPI (blue). Scale bars = 5 μm. (i-iii) Colocalization analysis of NCAPH (red curve) and p-H2AX (green curve) with DAPI (blue curve). The fluorescence intensity profiles of NCAPH and p-H2AX show the fluorescence distribution across the dotted line (x-axis). Fluorescence intensity is plotted along the y-axis. (D) Calculation of colocalization of GEN1 and p-H2AX fluorescence. For precise quantification, more than 40 cells captured images by fluorescence microscopy at least three different fields were analyzed using the Pearson correlation coefficient (PCC) and the Mander's overlap coefficient (MOC) measurement methods. Values are represented in the form of mean ± SEM. $***P < 0.0001$. Statistical analysis of data was obtained by one-way ANOVA followed by Bonferroni's multiple comparison analysis tests.

the relative fluorescence signal of GEN1, compared with that of p-H2AX, was decreased in NCAPH-depleted cells, whereas it was restored by Lenti-siR-NCAPH treatment (Fig. 5C). To determine how NCAPH regulates the localization of GEN1 to facilitate DNA damage repair, the degree of colocalization between the fluorophores of GEN1 and p-H2AX was measured using Pearson's correlation coefficient and Mander's overlap coefficient analyses. Although the immunofluorescence experiments showed that the colocalization of GEN1 with p-H2AX significantly decreased in NCAPH-depleted cells, both measurement methods confirmed that this decrease was recovered by Lenti-siR-NCAPH treatment (Fig. 5D). Thus, NCAPH acts as a regulator to recruit GEN1 to the chromatin and stabilize it to repair damage induced by DNA-ICLs.

DISCUSSION

This study adopted two approaches to better understand the function of condensin I, which maintains normal cell division and genomic stability by repairing DNA damage induced by DNA-ICLs in humans. One approach focused on analyzing expression patterns during cell cycle progression, with respect to the function of NCAPH in chromosome segregation in cisplatin- or MMC-induced DNA-ICLs. The other approach identified and established relationships between an interaction partner and NCAPH. Our results indicate that NCAPH responds rapidly to the damage caused by DNA-ICLs, limits UFB formation, and plays an essential role in proper chromosome segregation and cytokinesis during sister-chromatid separation. Furthermore, we confirm that the interaction between GEN1 and NCAPH in the chromatin was promoted by the induction of DNA-ICLs. Our results show that NCAPH provides GEN1 with access to the chromatin and helps to maintain its position in the chromatin. Thus, NCAPH acts as an essential regulator that recruits and stabilizes GEN1 in chromatin, wherein the NCAPH–GEN1 interaction repairs damage caused by DNA-ICLs. These results provide further insight into how condensin I links the processes that repair DNA damage.

The two metazoan condensin complexes, condensin I and II, play individual roles in chromosome compaction. Condensin I regulates the lateral compaction of mitotic chromosomes, whereas condensin II modulates chromosome shortening (Green et al., 2012; Shintomi and Hirano, 2011). Ultra-high resolved imaging and experimental Hi-C (Lee and Seo, 2021) data on mitotic chromosomes show that condensin II builds long chromatin loops, whereas condensin I forms smaller DNA compaction within the larger condensin II-mediated DNA compaction, suggesting its involvement in chromosome separation (Gibcus et al., 2018; Walther et al., 2018). Condensin I causes shortening of mitotic chromosomes even in the absence of condensin II, whereas condensin II is essential for the decatenation and formation of a straight chromosome axis (Elbatsh et al., 2019). Thus, condensin mediates chromosome condensation and proper chromosome segregation (Lamothe et al., 2020; Thadani et al., 2012), and resolves cellular DNA damage reactions (Lehmann, 2005). Data on the role of condensin in repairing damaged DNA show that condensin does not play an important role in DSB repair but rather interacts strongly with the PARP1-XRCC1 complex in single-strand break repair (Heale et al., 2006). However, condensin II does not affect G2/M checkpoint activation, and condensin II depletion only affects HR recovery in IR-induced DSBs. Condensin II participates in the HR repair of DSBs to maintain genomic integrity (Wood et al., 2008).

We hypothesized that condensin I maintains the chromatids in a stable state until cell division ends by recovering the DNA damage caused by DNA-ICLs. ICL is an adduct that forms in DNA, which inhibits the processes involved in DNA unwinding. The ICL removal process can be simplified into three major steps: (i) DNA repair-associated proteins are mobilized in response to ICL-induced cell cycle arrest; (ii) the ICL is excised from the DNA by nucleotide excision repair and Fanconi anemia-related proteins; and (iii) DSBs are restored by the induction of DNA-ICLs to HJs (Lopez-Martinez et al., 2016). To repair ICLs formed by cisplatin or MMC, HR must proceed, and the covalently linked intermediates between the sister chromosomes must be removed before anaphase proceeds for stable chromosomal separation (Sarbajna et al., 2014). We observed that MMC-induced DNA-ICLs significantly enhanced NCAPH expression at the site of DNA damage, as shown by increased expression of DNA damage markers. G2/M-phase arrest was increased and UFBs were formed in NCAPH-depleted cells with cisplatin-induced DNA-ICLs, leading to defective chromosome segregation and cytokinesis failure. NCAPH reacted sensitively to DNA lesions caused by DNA-ICLs, and ensured normal cell division by completely removing the remaining DNA strands to repair DNA damage until the cells separated into two daughter cells. This indicates the presence of an NCAPH-interacting protein whose expression strongly correlated with that of condensin I, as well as the major HR mechanisms underlying DNA-ICL repair.

In ICL repair, the activities of the XPF-ERCC1 complex and other structure-selective endonucleases (SSEs), termed HJ resolvases, act collaboratively in the processes of translesion DNA synthesis and HR-mediated DNA repair (Lopez-Martinez et al., 2016; Pichierri et al., 2002). These SSEs, including MUS81–EME1 (Chen et al., 2001), SLX1–SLX4 (Fekairi et al., 2009), and GEN1 (Ip et al., 2008), describe two distinct HJ resolution pathways in human cells. SLX1, MUS81–EME1, and Fanconi-associated nuclease 1 endonucleases are known to be involved in repairing ICLs; however, the underlying mechanisms of regulation remain unclear (Zhang and Walter, 2014). To our knowledge, no studies have explored the mechanisms by which condensin I repairs the damage caused by DNA-ICLs and its relationship to HJ resolvases. We found that NCAPH regulates DNA-ICL damage repair via cooperation with HJ resolvases. HJ resolvases are required to prevent the intertwinement of sister chromosomes, thus ensuring correct chromosome condensation when sister chromatids separate (Wechsler et al., 2011). GEN1 (Yen1) can resolve HJs before chromosome separation, the last point of mitosis (Dehé and Gaillard, 2017). In the absence of HJ resolvases (GEN1−/− knockout cells deficient of MUS81), anaphase bridges are formed that persist until the end of mitosis, and these HRs, known as UFBs, delay the cell cycle and cause large-scale cell death (Chan et al., 2018). Our results of the effects of NCAPH depletion are consistent with this process, and therefore, an association between NCAPH and HJ resol-

vases may be expected. We demonstrated that NCAPH physically interacts with GEN1 but not with MUS81. The NCAPH–GEN1 interaction in the chromatin was significantly increased by induced DNA-ICLs, suggesting that this interaction is essential for repairing DNA-ICLs. The absence of NCAPH restricted the localization of GEN1 in chromatin during the G2/M-phase, indicating that NCAPH is a regulator of the recruitment and stabilization of GEN1 at DNA damage sites. NCAPH may play an essential role in repairing DNA damage caused by ICLs by interacting with GEN1. In the absence of NCAPH, the expression of other components of condensin I in the cytoplasm, nucleus, and chromatin fractions decreased, but this did not significantly affect the expression of other components of condensin II. Collectively, these data demonstrate a close correlation between NCAPH and GEN1, and that the regulation of the recruitment and stabilization of GEN1 to the DNA damage site by NCAPH may be the mechanism through which condensin I rapidly detects and repairs the damage caused by DNA-ICLs. Although this study is limited, as the results were validated only in cell culture models, it identifies a binding protein of condensin I and suggests a novel DNA-ICL repair mechanism.

Our findings show that the recruitment of NCAPH and GEN1 to DNA damage lesions is essential for DNA damage repair and normal cell division. In the absence of NCAPH, GEN1 is not stably maintained in the chromatin to repair ICLs, leading to the formation of chromosome bridges, lagging chromosomes, and late cytokinesis failures. Significantly, the interaction between NCAPH and GEN1 repairs DNA-ICLs. When DNA damage is detected, NCAPH and GEN1 react rapidly to increase their interaction at the site of DNA damage. In particular, NCAPH is involved in the recruitment and stabilization of GEN1 to chromatin in the G2/M-phase, thereby completely removing the intertwined DNA strands to facilitate efficient cell division; this reveals a mechanism of repairing DNA damage caused by DNA-ICLs. This study therefore provides new insight into the maintenance of chromosome stability via complete chromosome segregation facilitated by a DNA-ICL repair mechanism involving condensin I and HJ resolvase. These findings offer a new foundation for exploring the potential link between condensin and chromosome stability in future research.

Note: Supplementary information is available on the Molecules and Cells website (www.molcells.org).

ACKNOWLEDGMENTS

This work was supported by grant No. NRF-2021R1A2C 200708811 from the National Research Foundation of Korea (NRF). We would like to thank Editage (www.editage.co.kr) for English language editing.

AUTHOR CONTRIBUTIONS

J.H.K. performed the experiments, carried out the data analysis, and wrote the manuscript. J.H.H. discussed the results and contributed to the manuscript revision. Y.Y. performed the reviewed experimental works. All of the authors discussed and approved the final manuscript.

CONFLICT OF INTEREST

The authors have no potential conflicts of interest to disclose.

ORCID

Jae Hyeong Kim https://orcid.org/0000-0003-4675-5305
Yuna Youn https://orcid.org/0000-0002-1026-6748
Jin-Hyeok Hwang https://orcid.org/0000-0002-5643-8461

REFERENCES

Bessho, T. (2003). Induction of DNA replication-mediated double strand breaks by psoralen DNA interstrand cross-links. J. Biol. Chem. *278*, 5250-5254.

Bittmann, J., Grigaitis, R., Galanti, L., Amarell, S., Wilfling, F., Matos, J., and Pfander, B. (2020). An advanced cell cycle tag toolbox reveals principles underlying temporal control of structure-selective nucleases. Elife *9*, e52459.

Blanco, M.G., Matos, J., and West, S.C. (2014). Dual control of Yen1 nuclease activity and cellular localization by Cdk and Cdc14 prevents genome instability. Mol. Cell *54*, 94-106.

Bredberg, A., Lambert, B., and Söderhäll, S. (1982). Induction and repair of psoralen cross-links in DNA of normal human and xeroderma pigmentosum fibroblasts. Mutat. Res. *93*, 221-234.

Chan, K.L., Palmai-Pallag, T., Ying, S., and Hickson, I.D. (2009). Replication stress induces sister-chromatid bridging at fragile site loci in mitosis. Nat. Cell Biol. *11*, 753-760.

Chan, Y.W., Fugger, K., and West, S.C. (2018). Unresolved recombination intermediates lead to ultra-fine anaphase bridges, chromosome breaks and aberrations. Nat. Cell Biol. *20*, 92-103.

Chan, Y.W. and West, S.C. (2014). Spatial control of the GEN1 Holliday junction resolvase ensures genome stability. Nat. Commun. *5*, 4844.

Chanboonyasitt, P. and Chan, Y.W. (2021). Regulation of mitotic chromosome architecture and resolution of ultrafine anaphase bridges by PICH. Cell Cycle *20*, 2077-2090.

Chen, E.S., Sutani, T., and Yanagida, M. (2004). Cti1/C1D interacts with condensin SMC hinge and supports the DNA repair function of condensin. Proc. Natl. Acad. Sci. U. S. A. *101*, 8078-8083.

Chen, G. and Deng, X. (2018). Cell synchronization by double thymidine block. Bio Protoc. *8*, e2994.

Chen, X.B., Melchionna, R., Denis, C.M., Gaillard, P.H.L., Blasina, A., Van de Weyer, I., Boddy, M.N., Russell, P., Vialard, J., and McGowan, C.H. (2001). Human Mus81-associated endonuclease cleaves Holliday junctions in vitro. Mol. Cell *8*, 1117-1127.

Ciccia, A., Constantinou, A., and West, S.C. (2003). Identification and characterization of the human mus81-eme1 endonuclease. J. Biol. Chem. *278*, 25172-25178.

Dardalhon, M. and Averbeck, D. (1995). Pulsed-field gel electrophoresis analysis of the repair of psoralen plus UVA induced DNA photoadducts in Saccharomyces cerevisiae. Mutat. Res. *336*, 49-60.

De Silva, I.U., McHugh, P.J., Clingen, P.H., and Hartley, J.A. (2000). Defining the roles of nucleotide excision repair and recombination in the repair of DNA interstrand cross-links in mammalian cells. Mol. Cell. Biol. *20*, 7980-7990.

Deans, A.J. and West, S.C. (2011). DNA interstrand crosslink repair and cancer. Nat. Rev. Cancer *11*, 467-480.

Dehé, P.M. and Gaillard, P.H.L. (2017). Control of structure-specific endonucleases to maintain genome stability. Nat. Rev. Mol. Cell Biol. *18*, 315-330.

Dej, K.J., Ahn, C., and Orr-Weaver, T.L. (2004). Mutations in the Drosophila condensin subunit dCAP-G: defining the role of condensin for chromosome condensation in mitosis and gene expression in interphase.

Genetics *168*, 895-906.

Eissler, C.L., Mazón, G., Powers, B.L., Savinov, S.N., Symington, L.S., and Hall, M.C. (2014). The Cdk/cDc14 module controls activation of the Yen1 holliday junction resolvase to promote genome stability. Mol. Cell *54*, 80-93.

Elbatsh, A.M.O., Kim, E., Eeftens, J.M., Raaijmakers, J.A., van der Weide, R.H., García-Nieto, A., Bravo, S., Ganji, M., Uit de Bos, J., Teunissen, H., et al. (2019). Distinct roles for condensin's two ATPase sites in chromosome condensation. Mol. Cell *76*, 724-737.e5.

Fekairi, S., Scaglione, S., Chahwan, C., Taylor, E.R., Tissier, A., Coulon, S., Dong, M.Q., Ruse, C., Yates, J.R., 3rd, Russell, P., et al. (2009). Human SLX4 is a Holliday junction resolvase subunit that binds multiple DNA repair/recombination endonucleases. Cell *138*, 78-89.

García-Luis, J., Clemente-Blanco, A., Aragón, L., and Machín, F. (2014). Cdc14 targets the Holliday junction resolvase Yen1 to the nucleus in early anaphase. Cell Cycle *13*, 1392-1399.

Georges, S.A., Biery, M.C., Kim, S.Y., Schelter, J.M., Guo, J., Chang, A.N., Jackson, A.L., Carleton, M.O., Linsley, P.S., Cleary, M.A., et al. (2008). Coordinated regulation of cell cycle transcripts by p53-Inducible microRNAs, miR-192 and miR-215. Cancer Res. *68*, 10105-10112.

Gibcus, J.H., Samejima, K., Goloborodko, A., Samejima, I., Naumova, N., Nuebler, J., Kanemaki, M.T., Xie, L., Paulson, J.R., Earnshaw, W.C., et al. (2018). A pathway for mitotic chromosome formation. Science *359*, eaao6135.

Green, L.C., Kalitsis, P., Chang, T.M., Cipetic, M., Kim, J.H., Marshall, O., Turnbull, L., Whitchurch, C.B., Vagnarelli, P., Samejima, K., et al. (2012). Contrasting roles of condensin I and condensin II in mitotic chromosome formation. J. Cell Sci. *125*, 1591-1604.

Grigaitis, R., Ranjha, L., Wild, P., Kasaciunaite, K., Ceppi, I., Kissling, V., Henggeler, A., Susperregui, A., Peter, M., Seidel, R., et al. (2020). Phosphorylation of the RecQ helicase Sgs1/BLM controls its DNA unwinding activity during meiosis and mitosis. Dev. Cell *53*, 706-723.e5.

Heale, J.T., Ball, A.R., Jr., Schmiesing, J.A., Kim, J.S., Kong, X., Zhou, S., Hudson, D.F., Earnshaw, W.C., and Yokomori, K. (2006). Condensin I interacts with the PARP-1-XRCC1 complex and functions in DNA single-strand break repair. Mol. Cell *21*, 837-848.

Hirano, T. (2012). Condensins: universal organizers of chromosomes with diverse functions. Genes Dev. *26*, 1659-1678.

Hirano, T. (2016). Condensin-based chromosome organization from bacteria to vertebrates. Cell *164*, 847-857.

Holliday, R. (2007). A mechanism for gene conversion in fungi. Genet. Res. *89*, 285-307.

Hustedt, N. and Durocher, D. (2016). The control of DNA repair by the cell cycle. Nat. Cell Biol. *19*, 1-9.

Ip, S.C., Rass, U., Blanco, M.G., Flynn, H.R., Skehel, J.M., and West, S.C. (2008). Identification of Holliday junction resolvases from humans and yeast. Nature *456*, 357-361.

Kim, J.H., Youn, Y., Kim, K.T., Jang, G., and Hwang, J.H. (2019). Non-SMC condensin I complex subunit H mediates mature chromosome condensation and DNA damage in pancreatic cancer cells. Sci. Rep. *9*, 17889.

Kosugi, S., Hasebe, M., Tomita, M., and Yanagawa, H. (2009). Systematic identification of cell cycle-dependent yeast nucleocytoplasmic shuttling proteins by prediction of composite motifs. Proc. Natl. Acad. Sci. U. S. A. *106*, 10171-10176.

Lamothe, R., Costantino, L., and Koshland, D.E. (2020). The spatial regulation of condensin activity in chromosome condensation. Genes Dev. *34*, 819-831.

Lee, H. and Seo, P.J. (2021). HiCORE: Hi-C analysis for identification of core chromatin looping regions with higher resolution. Mol. Cells *44*, 883-892.

Lehmann, A.R. (2005). The role of SMC proteins in the responses to DNA damage. DNA Repair (Amst.) *4*, 309-314.

Li, P., Jin, H., and Yu, H.G. (2014). Condensin suppresses recombination and regulates double-strand break processing at the repetitive ribosomal DNA array to ensure proper chromosome segregation during meiosis in budding yeast. Mol. Biol. Cell *25*, 2934-2947.

Li, X. and Heyer, W.D. (2008). Homologous recombination in DNA repair and DNA damage tolerance. Cell Res. *18*, 99-113.

Lopez-Martinez, D., Liang, C.C., and Cohn, M.A. (2016). Cellular response to DNA interstrand crosslinks: the Fanconi anemia pathway. Cell. Mol. Life Sci. *73*, 3097-3114.

Machín, F. (2020). Implications of metastable nicks and nicked Holliday junctions in processing joint molecules in mitosis and meiosis. Genes (Basel) *11*, 1498.

Matos, J., Blanco, M.G., Maslen, S., Skehel, J.M., and West, S.C. (2011). Regulatory control of the resolution of DNA recombination intermediates during meiosis and mitosis. Cell *147*, 158-172.

McHugh, P.J., Sones, W.R., and Hartley, J.A. (2000). Repair of intermediate structures produced at DNA interstrand cross-links in Saccharomyces cerevisiae. Mol. Cell. Biol. *20*, 3425-3433.

Niedernhofer, L.J., Odijk, H., Budzowska, M., van Drunen, E., Maas, A., Theil, A.F., de Wit, J., Jaspers, N.G., Beverloo, H.B., Hoeijmakers, J.H., et al. (2004). The structure-specific endonuclease Ercc1-Xpf is required to resolve DNA interstrand cross-link-induced double-strand breaks. Mol. Cell. Biol. *24*, 5776-5787.

Ono, T., Losada, A., Hirano, M., Myers, M.P., Neuwald, A.F., and Hirano, T. (2003). Differential contributions of condensin I and condensin II to mitotic chromosome architecture in vertebrate cells. Cell *115*, 109-121.

Pichierri, P., Averbeck, D., and Rosselli, F. (2002). DNA cross-link-dependent RAD50/MRE11/NBS1 subnuclear assembly requires the Fanconi anemia C protein. Hum. Mol. Genet. *11*, 2531-2546.

Redon, C., Pilch, D., Rogakou, E., Sedelnikova, O., Newrock, K., and Bonner, W. (2002). Histone H2A variants H2AX and H2AZ. Curr. Opin. Genet. Dev. *12*, 162-169.

Rothfuss, A. and Grompe, M. (2004). Repair kinetics of genomic interstrand DNA cross-links: evidence for DNA double-strand break-dependent activation of the Fanconi anemia/BRCA pathway. Mol. Cell. Biol. *24*, 123-134.

Sarbajna, S., Davies, D., and West, S.C. (2014). Roles of SLX1-SLX4, MUS81-EME1, and GEN1 in avoiding genome instability and mitotic catastrophe. Genes Dev. *28*, 1124-1136.

Shintomi, K. and Hirano, T. (2011). The relative ratio of condensin I to II determines chromosome shapes. Genes Dev. *25*, 1464-1469.

Thadani, R., Uhlmann, F., and Heeger, S. (2012). Condensin, chromatin crossbarring and chromosome condensation. Curr. Biol. *22*, R1012-R1021.

Thiriet, C. and Hayes, J.J. (2005). Chromatin in need of a fix: phosphorylation of H2AX connects chromatin to DNA repair. Mol. Cell *18*, 617-622.

Walther, N., Hossain, M.J., Politi, A.Z., Koch, B., Kueblbeck, M., Ødegård-Fougner, Ø., Lampe, M., and Ellenberg, J. (2018). A quantitative map of human Condensins provides new insights into mitotic chromosome architecture. J. Cell Biol. *217*, 2309-2328.

Wang, L.H., Mayer, B., Stemmann, O., and Nigg, E.A. (2010). Centromere DNA decatenation depends on cohesin removal and is required for mammalian cell division. J. Cell Sci. *123*, 806-813.

Wang, L.H., Schwarzbraun, T., Speicher, M.R., and Nigg, E.A. (2008). Persistence of DNA threads in human anaphase cells suggests late completion of sister chromatid decatenation. Chromosoma *117*, 123-135.

Wechsler, T., Newman, S., and West, S.C. (2011). Aberrant chromosome morphology in human cells defective for Holliday junction resolution. Nature *471*, 642-646.

Whitfield, M.L., Zheng, L.X., Baldwin, A., Ohta, T., Hurt, M.M., and Marzluff, W.F. (2000). Stem-loop binding protein, the protein that binds the 3' end of histone mRNA, is cell cycle regulated by both translational and posttranslational mechanisms. Mol. Cell. Biol. *20*, 4188-4198.

Wood, J.L., Liang, Y., Li, K., and Chen, J. (2008). Microcephalin/MCPH1 associates with the Condensin II complex to function in homologous recombination repair. J. Biol. Chem. *283*, 29586-29592.

Wyatt, H.D., Sarbajna, S., Matos, J., and West, S.C. (2013). Coordinated actions of SLX1-SLX4 and MUS81-EME1 for Holliday junction resolution in human cells. Mol. Cell *52*, 234-247.

Yu, H.G. and Koshland, D.E. (2003). Meiotic condensin is required for proper chromosome compaction, SC assembly, and resolution of recombination-dependent chromosome linkages. J. Cell Biol. *163*, 937-947.

Zhang, J. and Walter, J.C. (2014). Mechanism and regulation of incisions during DNA interstrand cross-link repair. DNA Repair (Amst.) *19*, 135-142.